

Is the Freeze Drying Method Effect on the Phase Transition Temperature of β/β' Lithium Zirconium Phosphate?

M. Ghasemnejad Esfahlan, S. M. Seyedahmadian*

Department of Chemistry, Azarbaijan Shahid Madani University, Tabriz, Iran.

Article history:

Received 2/7/2014

Accepted 15/8/2014

Published online 1/9/2014

Keywords:

Freeze Drying

Thermal Analyses

Lithium Ion Batteries

Phase Transition

Degree of Crystallinity

*Corresponding author:

E-mail address:

seyedahmadian@azaruniv.edu

Phone: +98 914 1170656

Fax: +98 4132 4327545

Abstract

Spherical granules of the superionic conductor β/β' $\text{LiZr}_2(\text{PO}_4)_3$ in the range of sub 100 nm size were synthesized via freeze drying method and fully reviewed in all aspects. Samples were characterized by the X-ray diffractometry (XRD), the Thermal analysis (TG, DSC), the Fourier Transform Infra-Red Spectroscopy (FTIR) and the Scanning Electron Microscopy (SEM). Their structure depends largely on the method of synthesis, thermal treatment, and conditions of storing samples. Degree of Crystallinity and phase purity in different annealing time were tested. The synthesis temperature does not exceed 873 K in any step of the synthesis. The low temperature phases (β with the $Pbna$ space group and β' with the $P2_1/n$ space group) were prepared at optimum condition. By the Differential Scanning Calorimetry it was shown the phase transition from $\beta \leftrightarrow \beta'$ occurred at about 567-597 K. The temperature of annealing the phosphate and calcination time is not very effective to phase transition temperature.

2014 JNS All rights reserved

1. Introduction

Batteries are important technology components in modern society. They are used to power electric and hybrid electric vehicles and to store wind and solar energy in smart grids. For these reasons batteries are of prime importance due to fast storage and use of energy. Each cell of a battery stores electrical energy as chemical energy in two electrodes, a reductant (anode) and an oxidant (cathode), separated by an electrolyte that transfers the ionic component of the chemical reaction inside

the cell [1]. Currently, liquid electrolytes such as LiClO_4 and LiPF_6 dissolved in ethylene carbonate (EC) and propylene carbonate (PC) are used in lithium ion batteries. These electrolytes suffer from many major limitations such as a limited temperature range of operation, device failure due to electrode corrosion by electrolyte solution and unsuitable shapes. A suitable solid electrolyte is required to overcome these disadvantages. Sodium (Na) Super Ion Conductor (NASICON) with the chemical formula $\text{Na}_{1+x}\text{Zr}_{2-x}\text{P}_{3x}\text{O}_{12}$ is a suitable

candidate for this propose. Originally these framework structures were reported by Goodenough and Hong in 1976 [2-4]. The general formula of NASICON composition can be written as $\text{AMM}(\text{PO}_4)_3$ where the site "A" can be occupied by alkali ions (Li^+ , Na^+ , K^+ , ...) and alkaline earth ions (Mg^{2+} , Ca^{2+} , Sr^{2+} , ...). The M and M' sites are occupied by Di (Zn^{2+} , Ni^{2+} , Mn^{2+} , ...), Tri (Fe^{3+} , Ti^{3+} , V^{3+} , ...), Tetra (Ti^{4+} , Zr^{4+} , ...), and Penta (V^{5+} , Nb^{5+} , Ta^{5+} , ...) valent transition metal-ions to balance the charge neutrality [5]. The ionic conductivity of these materials can be varied over a wide range due to possibility of substitution by different ions. Therefore, they can be used in many different applications such as low thermal expansion materials (Ca, Sr, Ba at the site A), insertion and extraction materials, immobilization of radioactive waste, catalyst supports (Cu and Ag NASICONs), sensors and ion selective electrodes, solid-state batteries and fuel cell devices [6-11]. The lithium-analogue of NASICON can contain the same basic zirconium phosphate anion framework as NASICON. However the smaller lithium cation introduces more degree of complexity to the system and results in the formation of four different polymorphs of $\text{LiZr}_2(\text{PO}_4)_3$ [12, 13]. Due to relatively high ionic conductivity and redox stability of the Zr, Ta and Ti containing compounds, lithium fast ion conductor with formula $\text{LiM}_2(\text{PO}_4)_3$, (M = Zr, Sn, Hf, Ta and Ti), has attracted the attention of many researchers. Moreover, the high-energy densities and high open circuit potentials of lithium based solid electrolytes makes them suitable to use in all solid state batteries [14-18]. Therefore, the superionic conductivities, thermodynamic and other physical properties of NZP ($\text{NaZr}_2(\text{PO}_4)_3$ -type structure) and $\text{LiZr}_2(\text{PO}_4)_3$ have been widely studied [13, 19-25]. When $\text{LiZr}_2(\text{PO}_4)_3$ is prepared at about

1473 K it results in α - $\text{LiZr}_2(\text{PO}_4)_3$ phase, which has a rhombohedral structure (similar to the sodium counterpart) and it becomes stable on cooling down to about 333 K undergoing a phase transition to the triclinically distorted α' phase at this point. Incredibly, the preparation of the materials around 1173 K does not yield α phase and instead a new orthorhombic polymorph, β - $\text{LiZr}_2(\text{PO}_4)_3$ is formed [26]. On cooling, this β polymorph undergoes a structural transition at about 573 K which leads to the formation of the monoclinically distorted β - $\text{LiZr}_2(\text{PO}_4)_3$ phase. Also the direct transformation between the high temperature and low temperature phases does not take place [27]. There exist many different routes for synthesis of solid materials, concerning the basic method, types of precursors and the medium used for the precursor preparation before reaction in the thermal treatment step (calcination) [28, 29]. Usually, many of these techniques lead to migration affects, separation of species, and loss of homogeneity in products. Water is an environment-friendly solvent and ice crystals porogens is green and sustainable materials [30]. Freeze drying or lyophilization is a novel process that can provide certain advantages and is capable of producing fine nano particles. In recent years, this method has been used as a unique and prominent route to produce novel materials [31]. The process is based on instant freezing of nebulized droplet (granules) of a precursor solution into stirred liquid nitrogen (77 K), resulting in solid frozen particles. This rapid freezing prevents phase segregation and minimizes ice crystal growth that can disturb homogeneity which occurs during conventional freezing of larger volume units. In the following, the frozen solvent is removed by sublimation. In this way, many problems which emerge in using other types of granulation methods such as granule

contraction, formation of hollows, strong inter particle bonds and migration of additives and etc. are avoided [32]. This method also is widely used in preparation of high purity ceramics, super conducting materials, biomedical materials, catalytic materials, hard alloys etc. [33]. Another aim of freeze drying is to produce materials with good shelf stability, which also depends very much on the last step of the process, namely, the packing and conditions of storage. To produce dry powders, the ice crystals are removed from the frozen droplets via sublimation in the lyophilization stage. The sublimation is carried out below the triple point of water (6 mbar, 273.16 K) to prevent melting ice crystals into liquid water that can destroy the solid structure of the nano-aggregates. As a result of using this procedure, the products have larger surface areas compared to those of the solid state methods [34, 35].

With regards to this sentence that their structure that depends on the method of synthesis, thermal treatment, and conditions of storing samples, the aim of this study is the synthesis and characterization of polymorphic NASICON-type $\text{LiZr}_2(\text{PO}_4)_3$ nano powders via freeze drying method and determination of the degree of crystallinity, structural and thermal analysis, calcination in different times and temperatures and studying its effects on the phase transition temperature of products.

2. Experimental procedure

2.1. Starting Materials and Preparation

Stoichiometry amounts of Citric acid 99.5% (Sigma-Aldrich), Zirconium (IV) oxynitrate hydrate 99% purity (Sigma-Aldrich), Lithium carbonate pure (Merck) and Ammonium dihydrogen phosphate 99% purity (Merck), with a molar ratio of 1:2:0.5:3 were dissolved in 100 ml deionized water, 50 ml Methanol and 10% excess lithium carbonate to prevent lithium

vaporization at high temperature step (calcination) with final stirring for 2 h at 353 K.

2.2. Freeze Drying

The prepared solution cooled down to room temperature and sprayed into liquid nitrogen (77 K). The frozen material dried in vacuum (10-20 mbars) at 203 K via a Zirbus Sublimator 400/II Freeze Dryer for about 24 h. Citric acid was used as the fuel and the binder. Starting materials were followed using thermogravimetric analysis (TG) by using a Mettler Toledo TGA/SDTA 851e with STARe software in the range of 323–1173 K at a heating rate of 10K/minute with a sensitivity of 0.02 mg.

2.3. Calcination

The materials were calcined at different times, namely, 6 h, 8 h, 10 h, 12 h and 20 h at 873 K for this low temperature phases (β , β'). Optimal condition with regards to XRD pattern and degree of crystallinity for low phases was selected at 873 K for about 10 h and 12 h, under Argon (99.99%) atmosphere in a tube furnace (Exciton EX 1200-15-6T).

2.4. Characterization Method

The products were characterized by the X-ray diffractometry (XRD), the Differential Scanning Calorimetry (DSC), the Fourier Transform Infra-Red Analysis (FTIR) and the Scanning Electron Microscopy (SEM). The XRD spectra were recorded for all the samples by using a Bruker D8 Advanced X-ray diffractometer with monochromatic $\text{Cu-K}\alpha$ radiation ($\lambda=1.54060 \text{ \AA}$) at glancing angles between 10° and 40° with step 0.040° and set time 2s. The Degree of Crystallinity of products was performed by Accelrys Materials Studio v6.0 software. The DSC measurements for these powders were carried out using a Mettler Toledo DSC 821e. The IR spectrum was recorded for each sample

in the range of 400 cm^{-1} to 2000 cm^{-1} at room temperature using a Bruker Vector 22 FTIR Spectrophotometer. The microstructure of the products (SEM) was investigated by VEGA TESCAN-XMU.

3. Results and discussion

3.1. Freeze Drying Technique and SEM Analysis

In this work nano-sized spherical shaped, $\text{LiZr}_2(\text{PO}_4)_3$ with size about sub 100 nm are synthesized as shown in Figure 1 (a, b). Freeze drying method has been already shown to get fine and homogeneous particle distributions. Several rewards support the choice of this procedure, namely, the homogeneous reactant distribution, the presence of a carbon source, and mild annealing temperatures. Freeze drying results in the high purity products.

3.2. Thermogravimetric Analysis

The TG curves for the starting mixture indicates that the latter water loss of hydration according to the water molecules, NH_3 and CO_2 are lost below 513 K. We observe marked distinctions in temperature range of condensing phosphate groups, for instance, the DTA peak at 553 K becomes stronger, which is attributed to the loss of excess Li from the mixture presumably as Li_2O and the curve shows a weak feature at 743 K is shown in Figure 2.

3.3. XRD Patterns and Calcination Times

To form the desired low temperature $\text{LiZr}_2(\text{PO}_4)_3$ materials, powders obtained from a freeze dryer were heated at 873 K for different times for 10 h and 12 h. Structural analysis of this low temperature phase shows the usual reflections corresponding to the NASICON-type structure, confirming a single NASICON-type $\text{LiZr}_2(\text{PO}_4)_3$ crystalline phase identical to β' phase is shown in Figure 3.

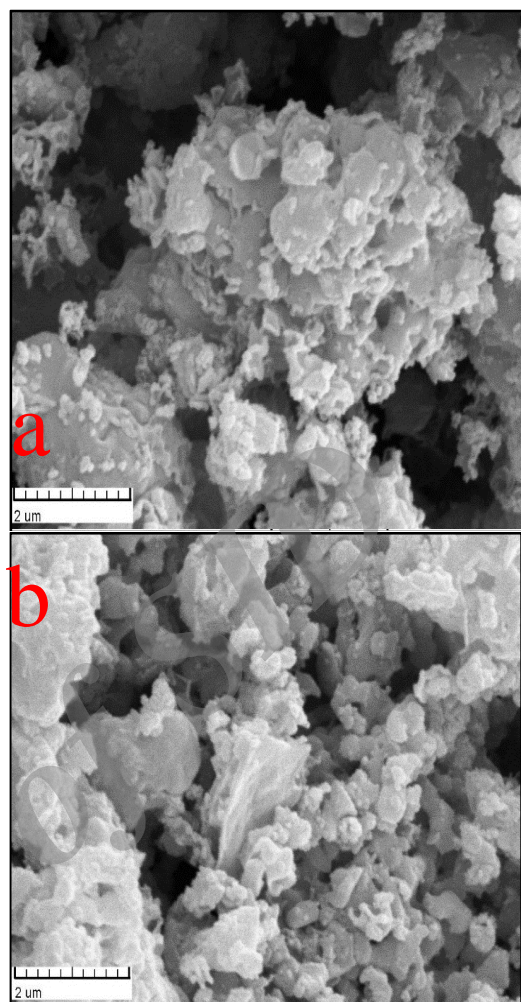


Fig.1. SEM image of sphere shaped powder $\text{LiZr}_2(\text{PO}_4)_3$ annealed at 873 K for (a) 10 h and (b) 12 h.

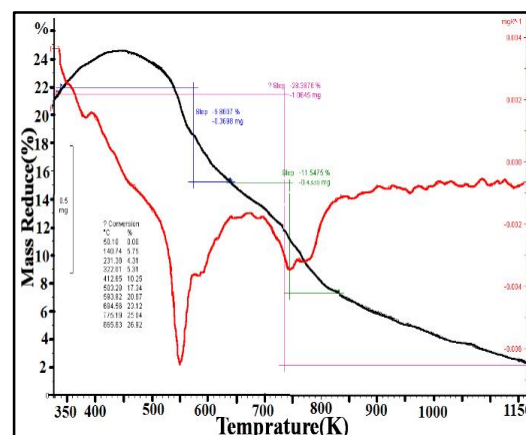


Fig.2. TG curve of the starting mixture.

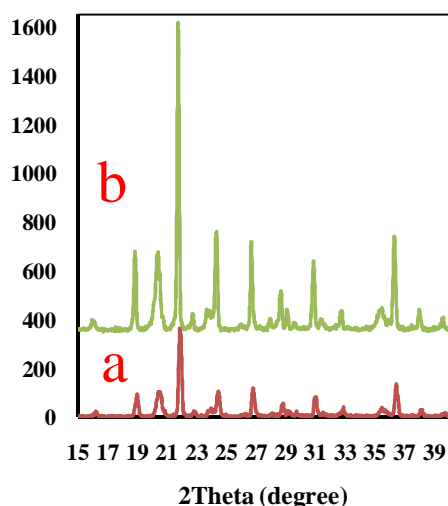


Fig.3. Room temperature XRD patterns from $\text{LiZr}_2(\text{PO}_4)_3$ powders annealed at 873 K for (a) 10 h and (b) 12 h.

3.4. DSC Studies

In DSC studies of these low temperature phases with annealing at 10 h and 12 h, curves show a single reproducible anomaly with hysteresis about 567 K corresponding to a first order transition from monoclinic to orthorhombic (start from 567 K, end 597 K) for both products as is shown in Figure 4 (a, b). However, the time of annealing is not very effective in the phase transition temperature. Casciola et al. reported this phase transition at about 543 K, Ruffo et al. at about 603 K and Catti et al. at about 573 K. In the temperature range of 567–597 K, the monoclinic and orthorhombic phases coexist in the XRD patterns [13, 22, 36-38].

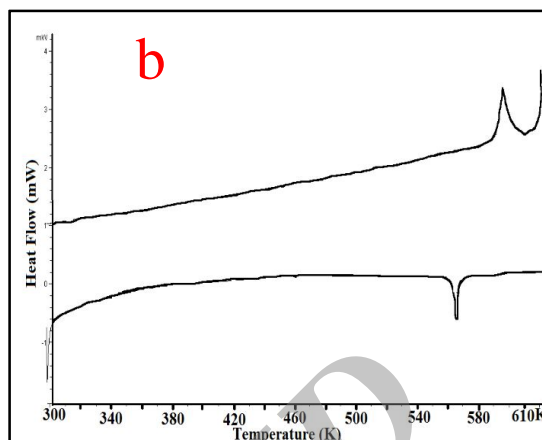
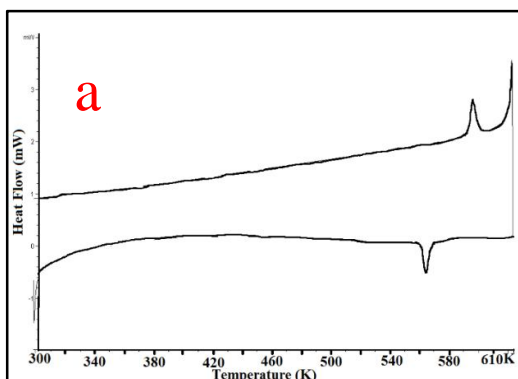


Fig.4. DSC studies of first order transition from monoclinic to orthorhombic phase that annealed at 873 K in 10 h (a) and 12 h (b).

3.5. FTIR Analysis

The vibrational spectroscopy provides valuable insight into the fundamental lithium intercalation reactions that attend in lithium insertion into $\text{LiZr}_2(\text{PO}_4)_3$. This the technique is extremely sensitive to small changes in the local structure of compounds[39]. The IR spectrum of $\text{LiZr}_2(\text{PO}_4)_3$ is shown in Figure 5. The band appearing at about 450 cm^{-1} can be attributed to symmetric stretching (γ_2) of $(\text{PO}_4)^{3-}$, whereas the bands around 600 and 1060 cm^{-1} is attributed to asymmetric stretching (γ_4 and γ_3) of $(\text{PO}_4)^{3-}$. Vibrations of PO_4 tetrahedral that correspond to two bending modes have been observed, i.e., bands at 430 cm^{-1} (γ_2) and 590 cm^{-1} (γ_4) are attributed to PO bending [39]. In the present study, all the characteristic bands for PO_4 vibrations are observed in the expected regions. This indicates that anion ring has not been distorted due to its coordination with cations of greater electronegativity [40].

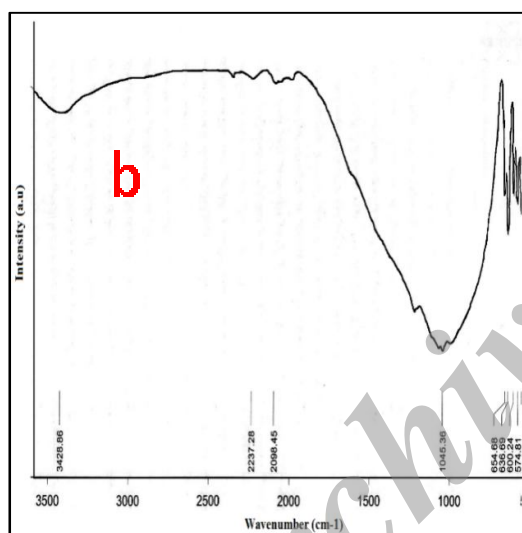
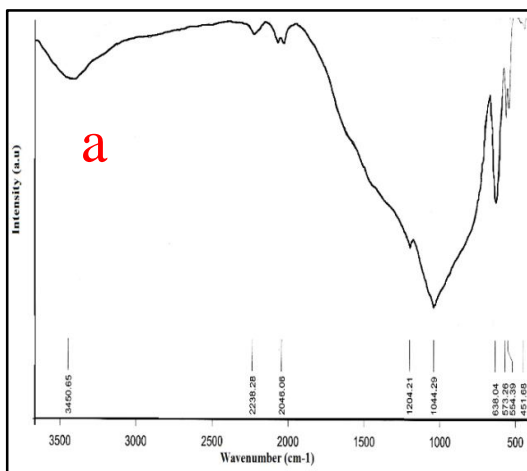


Fig.5. FTIR spectrum of $\text{LiZr}_2(\text{PO}_4)_3$ powders annealed at 873 K in 10 h (a) and 12 h (b).

3.6. Degree of Crystallinity

The degree of crystallinity (X_c), is the ratio between the total area of the crystalline diffraction peaks and the total area of the diffractogram. The degree of crystallinity calculated by Accelrys Materials Studio v6.0 software is shown in Table 1.

Table 1. Degree of Crystallinity of Low phases that calculated by Accelrys Materials Studio v6.0 software.

Sample	Low Temperature Phase	
	Time/h	Degree of Crystallinity/%
	6	80.13
	10	82.5
	12	80.4
	20	79.6

4. Conclusion

We reported here that the Freeze drying or lyophilization is a novel synthetic method in producing fine nano particles which can prevent many problems when using other types of synthetic methods in producing fine $\text{LiZr}_2(\text{PO}_4)_3$ nano powder. It also drastically reduces calcination time and temperature. We have prepared different polymorphs of $\text{LiZr}_2(\text{PO}_4)_3$ nano powders where the Differential Scanning Calorimetry study showed the phase transition for $\beta \leftrightarrow \beta'$ occurring at about 567-597 K. The temperature of phase transition depends on the synthesize method and temperature of annealing of the phosphate while the calcination time is not very effective on phase transition temperature.

Acknowledgment

The financial support from the Research Council of Azarbaijan Shahid Madani University is gratefully acknowledged.

References

- [1] J.B. Goodenough, K.-S. Park, J. Am. Chem. Soc., 135 (2013) 1167-1176.
- [2] J.B. Goodenough, Y. Kim, Chem. Mater., 22 (2009) 587-603.
- [3] F. Lalère, J.B. Leriche, M. Courty, S. Boulineau, V. Viallet, C. Masquelier, V. Seznec, J. Power Sources, 247 (2014) 975-980.

- [4] C. Masquelier, L. Croguennec, *Chem. Rev.*, 113 (2013) 6552-6591.
- [5] N. Anantharamulu, K. Koteswara Rao, G. Rambabu, B. Vijaya Kumar, V. Radha, M. Vithal, *J. Mater. Sci.*, 46 (2011) 2821-2837.
- [6] V.I. Pet'kov, A.V. Markin, N.N. Smirnova, *Russ. J. Phys. Chem. A*, 87 (2013) 1266-1271.
- [7] V.I. Pet'kov, E.A. Asabina, I.A. Shchelokov, *Inorganic Materials*, 49 (2013) 502-506.
- [8] K.B. Hueso, M. Armand, T. Rojo, *Energy & Environmental Science*, 6 (2013) 734-749.
- [9] O. Kamishima, K. Kawamura, T. Hattori, J. Kawamura, *J. Phys.: Condens. Matter*, 23 (2011) 225404.
- [10] J. Zheng, X. Li, Y. Yu, X. Feng, Y. Zhao, *J. Therm. Anal. Calorim.*, 117 (2014) 319-324.
- [11] W.-J. Ou, C.-S. Kao, Y.-S. Duh, J.-M. Hsu, *J. Therm. Anal. Calorim.*, 116 (2014) 1111-1116.
- [12] R.J. Brodd, in: *Batteries for Sustainability: Selected Entries from the Encyclopedia of Sustainability Science and Technology*, Springer Science+Business Media, New York, 2013, pp. 83.
- [13] K. Arbi, M.A. Paris, J. Sanz, *Dalton Trans.*, 40 (2011) 10195-10202.
- [14] F. Carn, M. Morcrette, B. Desport, R. Backov, *Solid State Sci.*, 17 (2013) 134-139.
- [15] G.R. Dahlin, K.E. Strxm, *Lithium Batteries: Research, Technology, and Applications*, Nova Science Publishers, New York, 2010.
- [16] B. Key, D.J. Schroeder, B.J. Ingram, J.T. Vaughey, *Chem. Mater.*, 24 (2011) 287-293.
- [17] D. Jugović, D. Uskoković, *J. Power Sources*, 190 (2009) 538-544.
- [18] J.W. Fergus, *J. Power Sources*, 195 (2010) 4554-4569.
- [19] S. Novikova, M. Sukhanov, M. Ermilova, N. Orekhova, A. Yaroslavtsev, *Inorganic Materials*, 48 (2012) 397-401.
- [20] A.A. Lizin, S.V. Tomilin, O.E. Gnevashov, A.N. Lukinykh, A.I. Orlova, *Radiochemistry*, 54 (2012) 542-548.
- [21] H. Xie, Y. Li, J.B. Goodenough, *RSC Advances*, 1 (2011) 1728-1731.
- [22] H. Xie, J.B. Goodenough, Y. Li, *J. Power Sources*, 196 (2011) 7760-7762.
- [23] V. Pet'kov, I. Shchelokov, A. Markin, N. Smirnova, M. Sukhanov, *J. Therm. Anal. Calorim.*, 102 (2010) 1147-1154.
- [24] V.I. Pet'kov, E.A. Asabina, M.V. Sukhanov, A.V. Markin, N.N. Smirnova, *Russ. J. Phys. Chem. A*, 87 (2013) 1960-1968.
- [25] V.I. Pet'kov, A.S. Shipilov, A.V. Markin, N.N. Smirnova, *J. Therm. Anal. Calorim.*, 115 (2014) 1453-1463.
- [26] D.W. Bruce, D. O'Hare, R.I. Walton, in: *Functional Oxides*, John Wiley and Sons, Padstow, 2010, pp. 157.
- [27] P.P. Kumar, S. Yashonath, *J. Chem. Sci. (Bangalore, India)*, 118 (2006) 135-154.
- [28] J. Orlenius, O. Lyckfeldt, K.A. Kasvayee, P. Johander, *J. Power Sources*, 213 (2012) 119-127.
- [29] Y. Cui, X. Zhao, R. Guo, *Electrochim. Acta*, 55 (2010) 922-926.
- [30] L. Qian, H. Zhang, *J. Chem. Technol. Biotechnol.*, 86 (2011) 172-184.
- [31] Y. Qiao, X. Wang, Y. Mai, X. Xia, J. Zhang, C. Gu, J. Tu, *Journal of Alloys and Compounds*, 536 (2012) 132-137.
- [32] W. Abdelwahed, G. Degobert, S. Stainmesse, H. Fessi, *Adv. Drug Delivery Rev.*, 58 (2006) 1688-1713.
- [33] X. Xi, G. Chen, Z. Nie, S. He, X. Pi, X. Zhu, J. Zhu, T. Zuo, *J. Alloys Compd.*, 497 (2010) 377-379.
- [34] W.S. Cheow, M.L.L. Ng, K. Kho, K. Hadinoto, *Int. J. Pharm.*, 404 (2011) 289-300.
- [35] A. Mousavi, A. Bensalem, B. Gee, *Green Chemistry Letters and Reviews*, 3 (2010) 135-142.
- [36] M. Catti, N. Morgante, R.M. Ibberson, *J. Solid State Chem.*, 152 (2000) 340-347.
- [37] M. Casciola, U. Costantino, L. Merlini, I.G.K. Andersen, E.K. Andersen, *Solid State Ionics*, 26 (1988) 229-235.
- [38] R. Ruffo, C.M. Mari, M. Catti, *Ionics*, 7 (2001) 105-108.
- [39] C.M. Burba, R. Frech, *Solid State Ionics*, 177 (2006) 1489-1494.
- [40] T. Savitha, S. Selvasekarapandian, C.S. Ramya, M.S. Bhuvaneshwari, G. Hirankumar, R.

Baskaran, P.C. Angelo, Journal of Power Sources, 157 (2006) 533-536.

Archive of SID